Journal of Statistical Mechanics: Theory and Experiment
An IOP and SISSA journal

The asymptotic properties of random strength and compliance of single-walled carbon nanotubes using atomistic simulation

Baidurya Bhattacharya[1] **and Qiang Lu**[2]

[1] Department of Civil Engineering, Indian Institute of Technology, Kharagpur, WB 721302, India
[2] Department of Mechanical Engineering, Northwestern University, Evanston, IL 60208, USA
E-mail: baidurya@iitkgp.ac.in and q-lu@northwestern.edu

Received 13 February 2006
Accepted 31 May 2006
Published 30 June 2006

Online at stacks.iop.org/JSTAT/2006/P06021
doi:10.1088/1742-5468/2006/06/P06021

Abstract. Mechanical response of deformable bodies is often concerned with either the sum or the extreme of an underlying random process. This paper investigates the asymptotic statistical properties of ultimate strength (σ_u) and compliance (C) of single-walled nanotubes (SWNTs) containing random defects using the technique of atomistic simulation (AS). The defects considered are of the Stone–Wales (SW) kind and a Matern hard-core random field applied on a finite cylindrical surface is used to describe the spatial distribution of the SW defects. A nanotube can be viewed as consisting of nominally identical segments of equal length possessing a stationary distribution of ultimate strength, σ_u. Under a weak dependence condition among the segment strengths (that decay to zero with increasing distance between the segments), consistent with the non-local nature of atomic interactions, formalized here in the form of strong mixing, the asymptotic properties of σ_u (as the extreme of the strong mixing sequence) and C (as the sum of a related strong mixing sequence) are studied with increasing tube length, l. The extremal index, measuring the stochastic dependence in the strength field, is estimated. We simulate a set of displacement controlled tensile loading up to fracture of (6, 6) SWNTs with length between 49 and 492 Å. With increasing l, the distribution of σ_u is found to shift to the left and become narrower and appears to fit the Weibull distribution rather well; the compliance of the tube increases with increasing l and becomes asymptotically normal. The compliance

1742-5468/06/P06021+21$30.00

and strength of the tube are found to become asymptotically uncorrelated. These results appear to validate the strong mixing property of the strength field.

Keywords: defects (theory), fracture (theory), random/ordered microstructures (theory), stochastic processes (theory)

Contents

1. Introduction

1.1. Statistics of material response

All real materials have defects. Depending on the scale in consideration, such defects may have significant effects on mechanical properties. Consider a deformable body Ω bounded by the surface $\partial\Omega$. A large class of problems in mechanical behaviour of materials can be modelled by assuming Ω to consist of a two-phase material—say the matrix (phase 1) and defects (phase 2) embedded in the matrix. The defects are distributed randomly in the matrix according a spatial process, Π. The spatial distribution of these defects is not too dense, such that almost surely no more than one defect is present in a small neighbourhood around any given point, $\underline{z}$. Also, the number of defects in any bounded region $A \subset \Omega$ is finite. Depending on the process in which the material is manufactured or assembled, the spatial density of the defects may not be uniform across the volume of the material; in other words, this point process is not necessarily homogeneous.

In the special case when the numbers of defects in non-overlapping regions are independent, the process Π can be modelled as a spatial Poisson process in state space $\mathbf{R}^3$ with mean measure, $\mu(B) = \int_B \lambda(\underline{z})\,\mathrm{d}\underline{z}$, where B is a bounded set in $\mathbf{R}^3$ and $\lambda(\underline{z})$ is the intensity of the process. The Poisson assumption is clearly violated, however, when factors such as finite size of defects, coalescence of several defects into one defect, or the disintegration of one defect into several etc are considered.

J. Stat. Mech. (2006) P06021

At the initial time t_0 the domain Ω and every region within it are in thermodynamic equilibrium, i.e., unless acted on by external agents, the domain Ω, its subsets, including the set of defects, do not evolve in time.

Now consider the properties of the defects. A defect at location $\underline{z}$ may be characterized at time t by a set of properties (i.e. marks), $\underline{\Theta}(\underline{z}, t)$, that, depending on the application of interest, could variously include its volume, surface area, density, orientation, elastic modulus, ultimate strength, damage state, nearest-neighbour distance, etc. In general, $\underline{\Theta}(\underline{z}, t)$ is random in nature. Even if at the initial time t_0 the field $\underline{\Theta}(\underline{z}, t_0)$ is homogeneous, due to the effect of the external actions, at later times $\underline{\Theta}(\underline{z}, t)$ becomes non-stationary in time as well as in space. It is likely that the elements of $\underline{\Theta}(\underline{z}, t)$ at any given $\underline{z}, t$ are dependent on each other.

We thus have a marked process $\mathbf{M}(t) = \{\underline{z}(t), \Theta(\underline{z}, t)\}$ with state space,

$$S(t) = \mathbf{R}^3 \times X \tag{1}$$

where X is the range of the random variables, $\underline{\Theta}$. Equation (1) emphasizes that $S(t)$, the state space of $\mathbf{M}(t)$, may evolve with time owing to some external action $E(t)$, for example, when Ω is subjected to loading. Hence there is a function $g(E(t))$ that maps $S(t_1)$ into $S(t_2), t_2 > t_1$. For example, the location of a defect may change owing to migration, the shape of the defect may change causing its surface area and volume to change, and so on.

Again, in the special case, when (i) $\Pi(t)$ is Poisson, (ii) $\underline{\Theta}(\underline{z}, t)$ is independent of $\Pi(t)$, (iii) $\underline{\Theta}(\underline{z}_1, t)$ and $\underline{\Theta}(\underline{z}_2, t)$ are independent for two distinct points $\underline{z}_1 \neq \underline{z}_2$ at all t, and (iv) the mapping g does not produce an atom, i.e. it does not pile distinct points of $S(t_1)$ on a single point of $S(t_2)$, then $\mathrm{M}(t)$ is a Poisson process [1].

Independence between marks at two different locations and between the marks and the point process, as often considered, is too restrictive since, in general, $\underline{\Theta}(\underline{z}, t)$ is influenced by past and present values of the marks throughout Ω. It is more reasonable to suppose that the influence decreases with increasing separation in space and time. This dependence structure may be formalized with suitable conditions. For now it suffices to say that knowledge about the mapping function g and the dependence structure of $\underline{\Theta}$ is crucial to understanding the mechanical behaviour of materials.

Consider some important property, $R(\underline{z}, t)$, of the defects. For simplicity, assume that R is a scalar and is either a constituent of $\underline{\Theta}$, or, more generally, a function of $\underline{\Theta}$. Let the randomness in the matrix be negligible compared to that of R so that the randomness in material response is governed by $R \ldots$. Let us concentrate on a volume element ΔV around $\underline{z}$ in Ω and time t such that it contains $N(\Delta V(\underline{z}))$ defects. Let R_i be the response of the ith defect located at $\underline{z}_i$.

Stochastic modelling of material response quite often boils down to looking either at sums (or, equivalently, averages) or at the extremes of the process $R(\underline{z}, t)$ (or some function f or h, respectively, of R) over ΔV. The former leads to bulk or globally averaged properties such as stiffness, while the latter leads to strength properties sensitive to local features such as fracture strength.

The average property at time t can be given by

$$Y_{\mathrm{ave}}^{\Delta V} = \frac{1}{N(\Delta V(\underline{z}))} \sum_{i=1}^{N(\Delta V(\underline{z}))} f(R_i). \tag{2}$$

J. Stat. Mech. (2006) P06021

Since mechanical failure is often governed by the criterion that the relevant material property is less than its critical value for the first time in (t_0,t) anywhere in Ω (see, e.g., [2]), the extreme property mentioned above is

$$Z_{\min}^{\Delta V} = \min[h(R_i); 0 \leq i \leq N(\Delta V(\underline{z}))]. \tag{3}$$

In this paper, we investigate the asymptotic properties of the extreme and the sum of processes related to R at the atomistic scale and how they affect material response and failure. The subject chosen for this is the single walled carbon nanotube with finite sized defects on its surface. A nanotube may be considered to be composed of n segments of length Δ_i for $i = 1, \ldots, n$. The length of the tube, $l_n = \sum_{i=1}^{n} \Delta_i$, depends on n; so do its strength, $W_{(n)}$, as the minimum of the sequence $\{W_n\}$ of individual segment strengths, and its compliance, $C_{(n)}$, as the sum of a related sequence, $\{C_n\}$.

It is reasonable to assume that the the strength random field in the tube is stationary and statistically dependent (owing to the non-local nature of atomic interactions) such that the dependence falls off with increasing separation among the segments. This decaying dependence structure will be formalized by a *strong mixing* condition applied to minima of stationary sequences in section 3.1.

The above representation allows us (i) to cast the problem as one dimensional in space, and (ii) to investigate the asymptotic properties and the asymptotic independence of $W_{(n)}$ and $C_{(n)}$ as n grows large, as described in sections 3.2 and 3.3.

Importantly, the *extremal index*, a number between 0 and 1 that measures the amount of statistical dependence in a random sequence and is potentially a very practical tool in determining the distribution of extrema of a dependent sequence, will be defined and determined for the random strength field. The extremal index allows one to build up on the rich collection of results from classical extreme value analysis of i.i.d. (independent and identically distributed) random variables, and in this case can help avoid costly numerical simulations for predicting the strength distribution of longer tubes.

The mechanical response of the nanotubes, necessary for finding their strength and compliance, is modelled using atomistic simulation, described next.

1.2. Carbon nanotubes and their mechanical properties

Carbon nanotubes (CNTs) are one or more layers of helical carbon microtubules, in which each layer can be described as rolling a single sp^2 graphene sheet into a cylinder along a vector called the chiral vector (m, n). Although earlier findings related to the tubular shape of carbon atoms had been reported, it was Iijima's [3] report that gave rise to the current wave of enthusiasm about CNTs. CNTs can be classified as single-walled nanotubes (SWNTs) and multi-walled nanotubes (MWNTs). MWNTs usually have diameters of less than 100 nm, and lengths in micrometres [3]–[6]. Various techniques, such as arc-discharge, laser-ablation, and catalytic growth, are applied to produce CNTs.

The study of carbon nanotubes has been motivated largely due to their extraordinary electronic, mechanical, and optical properties [7]–[9]. The combination of high stiffness, high strength, and good ductility with unique electronic properties (e.g., CNTs can be metallic or semiconducting depending on chirality) make the carbon nanotube a potentially very useful material. CNTs are now used as fibres in composites, scanning probe tips, field emission sources, electronic actuators, sensors, lithium ion and hydrogen

J. Stat. Mech. (2006) P06021

storage, and other electronic devices. Also, CNTs can be coated or doped to alter their properties for further applications.

A survey of recent results on the elastic modulus and strength of single-walled and multi-walled carbon nanotubes (SWNTs and MWNTs) has been reported in Lu and Bhattacharya [10]. The collected data clearly show the strength to vary between 5 and 150 GPa; elastic modulus and failure strain also show significant variation. Such variation has also been noticed in a few recent studies [11, 12]. An analytical understanding of these variations, their sources and how they can be controlled is essential before CNTs and CNT-based products can be considered for widespread use across industries.

Defects such as vacancies, metastable atoms, pentagons, heptagons, Stone–Wales (SW or 5–7–7–5) defects, heterogeneous atoms, discontinuities of walls, distortion in the packing configuration of CNT bundles, etc are widely observed in CNTs [4, 13, 14]. Such defects can be the result of the manufacturing process itself: according to an STM observation of the SWNT structure, about 10% of the samples were found to exhibit stable defect features under extended scanning [15]. Defects can also be introduced by mechanical loading and electron irradiation.

1.3. The Stone–Wales defect

The Stone–Wales (SW) defect, which is the focus of this paper, is composed of two pentagon–heptagon pairs, and can be formed by rotating a sp^2 bond by 90° (SW rotation). SW defects are stable and often present in carbon nanotubes, and are believed to play important roles in the mechanical, electronic, chemical, and other properties of carbon nanotubes. For example, Chandra *et al* [11] found that the SW defect significantly reduced the elastic modulus of single-walled nanotubes. Lu and Bhattacharya [16] investigated the role of one SW defect (located at the midsection of an armchair SWNT) on tensile properties over a range of loading speeds, and found that the presence of the defect significantly affects ultimate strength as well as ultimate strain at all loading speeds; the effect of the defect on stiffness is much less. Mielke *et al* [17] compared the role of various defects (vacancies, holes, and SW defects) in fracture of carbon nanotubes, and found that various one- and two-atom vacancies can reduce the failure stresses by 14–26%. The SW defects were also found to reduce the strength and failure strain, although their influence was less significant than vacancies and holes.

It has been found that SWNTs, under certain conditions, respond to the mechanical stimuli via the spontaneous formation of the SW defect beyond a certain value of applied strain around 5%–6% [18]. More interestingly, the SW defect can introduce successive SW rotations of different C–C bonds, which lead to gradual increase of tube length and shrinkage of tube diameter, resembling the necking phenomenon in tensile tests at macro-scale. This process also gradually changes in chirality of the CNT, from armchair to zigzag direction. This whole response is plastic, with necking and growth of a 'line defect', resembling the dislocation nucleation and moving in plastic deformation of a crystal in many ways. Yakobson [19] thus applied dislocation theory and compared the brittle and ductile failure paths after the nucleation of the SW defect.

The formation of SW defects due to mechanical strains has also been reported by other groups of researchers. In their atomistic simulation study, Liew *et al* [20] showed that SW defects formed at 20–25% tensile strain for single-walled and multi-walled nanotubes

J. Stat. Mech. (2006) P06021

with chirality ranging from (5, 5) to (20, 20). The formation of SW defects explained the plastic behaviour of the stress–strain curve. They also predicted failure strains of these tubes to be about 25.6%. A hybrid continuum/atomistic study by Jiang *et al* [21] reported the nucleation of SW defects both under tension and torsion. The reported SW transformation critical tensile strain is 4.95%, and critical shear strain is 12%. The activation energy and formation energy of the SW defect formation are also studied and related to the strength of the nanotube [22]–[24]. The nucleation of SW defects was found to depend on the tube chiralities, diameters and external conditions such as temperature.

2. Incorporating random Stone–Wales defects in SWNT mechanics

To our knowledge, there are few published works to date that study the effects of random defects on the mechanical properties of CNTs. The study by Saether [25] investigated the transverse mechanical properties of CNT bundles subject to random distortions in their packing configuration. This distortion, quantified by a vector describing the transverse displacement of the CNTs, may be caused by packing faults or inclusions. The magnitude and direction of the vector were both uniform random variables. The transverse moduli of CNT bundles were found to be highly sensitive to small distortions in the packing configuration. In another instance, Belavin *et al* [26] studied the effect of random atomic vacancies on the electronic properties of CNTs. More recently, Lu and Bhattacharya [10] conducted a systematic atomistic simulation-based study of randomly occurring SW defects on tensile properties of armchair as well as zigzag SWNTs.

Since there is not enough information in the experimental literature to provide a clear picture of statistics of SW defects (e.g. location, density, clustering tendency, etc), it is reasonable to start with the assumption that the defects occur in a completely random manner, which implies an underlying homogeneous Poisson spatial process [10]. We also acknowledge the fact that the SW defect is not a point defect but has a finite area and there should be no overlap between neighbouring defects. Therefore, we adopt a *Matern hard-core* point process [27] for the defect field. We emphasize that the Matern process has the property that any two points are at least h apart. The intensity of the Matern hard-core process is $\lambda_h = p_h\lambda$, where λ is the intensity of the underlying homogeneous Poisson point process and p_h is the probability that an arbitrary point from the underlying Poisson process will survive the Matern thinning. Thus, the average number of SW defects on an area A_t is $\lambda_h A_t$.

For a finite tube of length b, the probability p_h can be computed as [28]

$$p_h = \frac{1}{b}\int_0^b \frac{1-\mathrm{e}^{-\lambda A(y)}}{\lambda C(y;h)}\,\mathrm{d}y \tag{4}$$

where C is the area over which a Poisson point at (x_0, y_0) searches for its neighbours:

$$C(y_0;h) = \begin{cases} C'(y_0;h) & y_0 < h \\ \pi h^2 & h < y_0 < b-h \\ C''(y_0;h) & h < y_0 < b-h \end{cases} \tag{5}$$

with $C'(y_0;h) = h^2\left((\pi/2) + \theta + \frac{1}{2}\sin 2\theta\right), 0 < y_0 < h$ where $\theta = \arcsin y_0/h$. $C''(y_0;h)$ in equation (5) can be given simply by replacing $\theta = \arcsin(b-y_0)/h$ in the expression for C'.

J. Stat. Mech. (2006) P06021

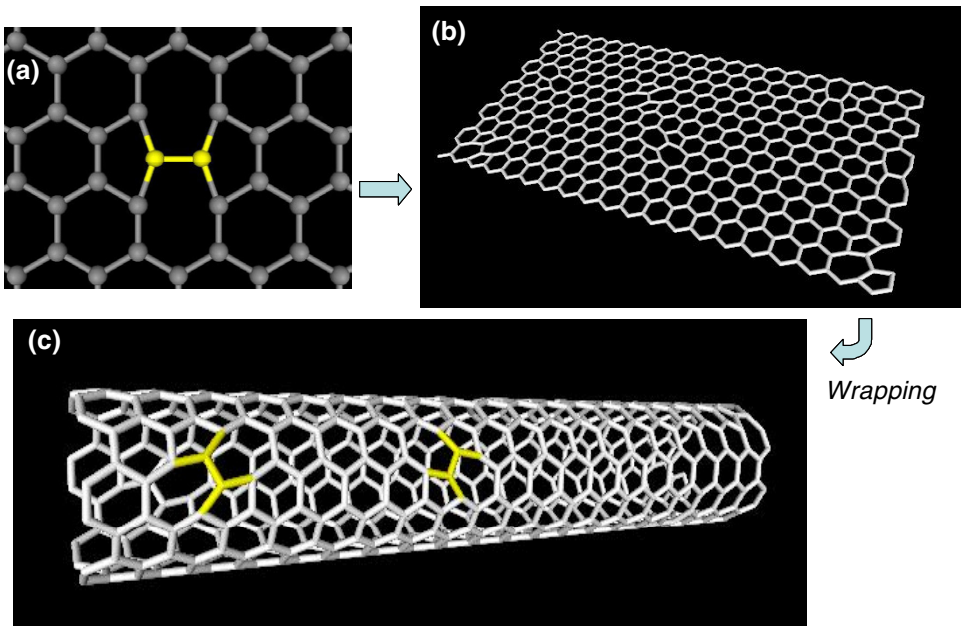

Figure 1. (a) A Stone–Wales defect with the rotated bond highlighted, (b) a graphene sheet with seven SW defects, and (c) the same sheet wrapped to form a (6, 6) SWNT; two SW defects are highlighted.

With the equilibrium sp^2 C–C bond length being 1.42 Å, the major axis diameter of a Stone–Wales defect is about 7.1 Å. Based on this, we conservatively fix the minimum-neighbour distance h of the Matern process at 8.0 Å.

The detailed procedure of generating SW defects has been provided in [28]. Once the location of the SW defect is selected, the sp^2 bond closest to the defect point is found, and then the bond is rotated by 90° to form an SW defect. Randomly occurring SW defects can thus be located on a graphene sheet, which in turn can be wrapped to produce the corresponding SWNT (figure 1).

For the atomistic simulation part of this study, a modified Morse potential model for describing the interaction among carbon atoms [29] is applied. This potential model does not have some of the shortcomings of the bond order potential models [30, 31]. The potential energy has the form

$$E_i = E_{\text{stretch}} + E_{\text{angle}} = \sum_j E_{\text{stretch}}(i,j) + \sum_{jk} E_{\text{angle}}(i,j,k) \tag{6}$$

$$E_{\text{stretch}}(i,j) = D_e\{[1 - \mathrm{e}^{-\beta(r-r_0)}]^2 - 1\} \tag{7}$$

$$E_{\text{angle}}(i,j,k) = \tfrac{1}{2}k_\theta(\theta_{ijk} - \theta_0)^2[1 + k_{\text{sextic}}(\theta_{ijk} - \theta_0)^4]. \tag{8}$$

This is the usual Morse potential except that the bond angle-bending energy has been added and the constants are slightly modified so that it corresponds with the Brenner potential [32] for strains below 10% [29]. E_{stretch} in equation (6) is the potential energy due to bond strength; r is the length of the bond. E_{angle} in equation (6) is the potential energy due to the bond angle bending; θ is the current angle of the adjacent bonds. The potential model parameters are $r_0 = 1.39 \times 10^{-10}$ m, $D_e = 6.031\,05 \times 10^{-19}$ N m,

J. Stat. Mech. (2006) P06021

Table 1. Reduced units for atomistic simulation.

Quantity	Reduced units	Real units
Length	1	1×10^{-10} m
Energy	1	$eV = 1.602 \times 10^{-19}$ J
Mass	1	1.992×10^{-26} kg
Temperature	1	1.1609×10^{4} K
Time	1	3.526×10^{-14} s
Force	1	1.602×10^{-9} N
Pressure	1	160.2 GPa
Speed	1	2.836×10^{3} m s^{-1}

$\beta = 2.625 \times 10^{10}$ m^{-1}, $\theta_0 = 2.094$ rad, $k_\theta = 0.9 \times 10^{-18}$ N m rad^{-2}, $k_{\text{sextic}} = 0.754$ rad^{-4}. For computational convenience, time, distance, and quantities representing velocity, energy, etc are reduced to non-dimensional numbers during the simulation. Table 1 shows the reduction of units.

We adopt the cut-off distance (r_c) as well as the critical inter-atomic separation (r_f) as $r_f = r_c = 1.77$ Å in this paper. The distance between neighbouring carbon atoms on the graphene sheet, a_0, is 1.42 Å, which is the C–C sp^2 bond length in equilibrium. The initial atomic positions are obtained by wrapping a graphene sheet into a cylinder along the chiral vector $\mathbf{C}_n = m\mathbf{a}_1 + n\mathbf{a}_2$ such that the origin (0, 0) coincides with the point (m, n). The tube diameter is thus obtained as $d = a_0\sqrt{3(m^2 + n^2 + mn)}/\pi$.

The initial atomic velocities are randomly chosen according to a uniform distribution (between the limits −0.5 and 0.5) and then rescaled to match the initial temperature (300 K in this example). The mechanical loading is applied through moving the atoms at both ends away from each other at constant speed without relaxing until fracture occurs.

In order to study the asymptotic behaviour of strength and compliance, we start with a single-walled nanotube (SWNT) in (6, 6) armchair configuration. The tube diameter is 8.14 Å. The length, l, of the tube is 49.2 Å. The total number of atoms in the simulation is 480. A typical time history of tensile loading to fracture generated for such a tube is shown in 2.

Benchmarking studies investigating the tensile and fracture behaviour of such simulations have already been reported in the literature [16, 10, 33, 34]. It has been found that there is no discernible yield point and fracture of SWNTs is always catastrophic, although a crack-length dependence on fracture resistance has been found. In originally defect free tubes, fracture initiates at completely random locations on the tube, meaning that there is no preferential location such as the ends or the mid-section. With the introduction of defects, fracture always initiates at a defect, and the stiffness and ultimate strength as well as ductility (measured as ultimate strain) reduce as a result. The strain rate effect on these mechanical properties has also been studied: over a range of four orders of magnitude in loading speed, strength as well as ductility, and to a lesser extent stiffness, showed a marked upward trend with increasing loading speed.

Figure 3 shows the first two moments of SWNT ultimate strength as a function of the average number of SW defects on the tube. For each average number of defects, 33 SWNTs were analysed. The average number of defects in figure 3 ranges from 0 to 3.9. Zero average defects imply a defect-free tube. The next higher value of 0.9 is arrived at

J. Stat. Mech. (2006) P06021

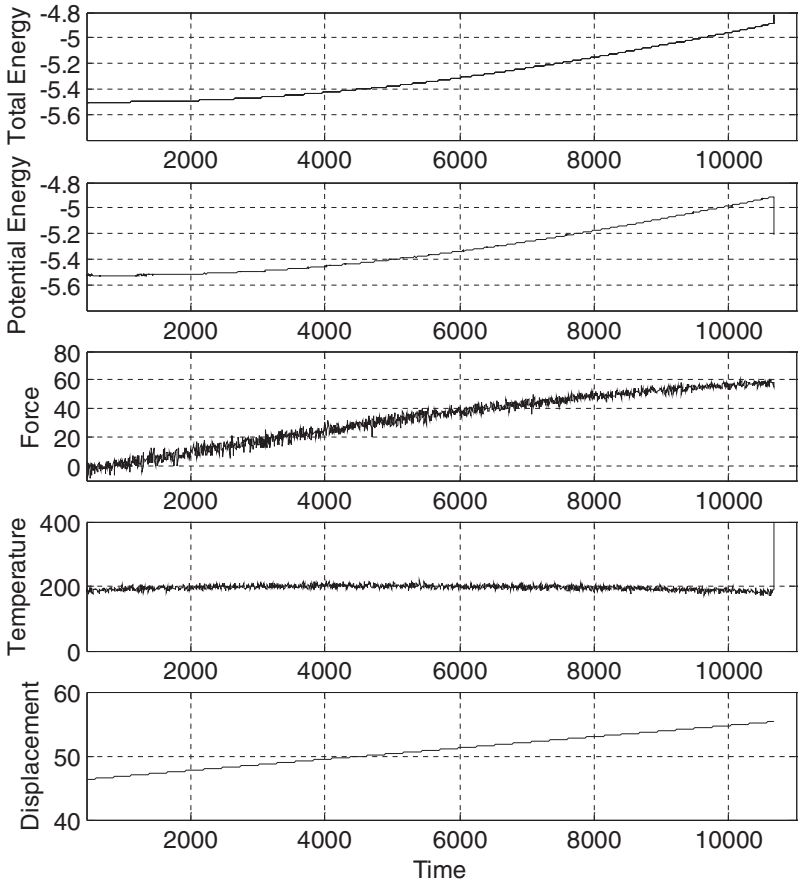

Figure 2. A typical set of time history generated for tensile loading up to fracture of a (6, 6) SWNT of length 46.3 Å with loading speed 5 nm ns^{-1} at temperature around 200 K.

thus: we start with $\lambda = 0.8 \times 10^{-3}$ Å^{-2} as the rate of the underlying Poisson field; this value of λ produces an average of one P point on the tube, and after the Matern thinning imposed by $h = 8.0$ Å leaves an average of 0.9 SW defects on the same tube. The value of 3.9 average defects corresponds to $\lambda = 4.8 \times 10^{-3}$ Å^{-2}.

The strength variability in the absence of any defect (zero average defects) in figure 3 is interesting: it arises solely from thermal fluctuations. The ultimate strength is calculated at the maximum force point, $\sigma_u = F_{\max}/A_0$, where F is the maximum axial force and A_0 is the cross section area assuming the thickness of tube wall is 0.34 nm. The tube compliance is determined as the reciprocal of the initial stiffness, E. The initial stiffness is determined by first fitting a quadratic curve between the initial portion of the potential energy, P, versus axial deformation, x (up to the point corresponding to 3.48% axial strain), as $P = ax^2$. The initial stiffness is linearly related to the parameter a through the initial geometry of the tube.

The asymptotic behaviour of strength and compliance of the tubes with increasing length will be taken up in the next section.

J. Stat. Mech. (2006) P06021

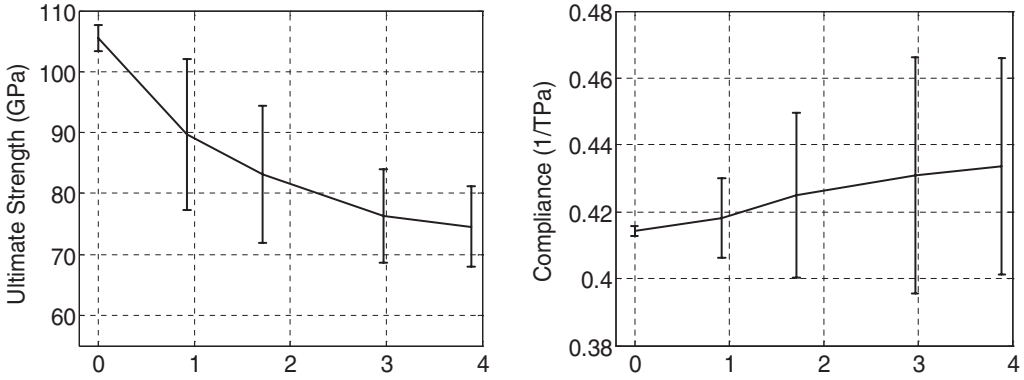

Figure 3. Statistics of SWNT ultimate strength and compliance as a function of average number of defects on the tube (dashed line = mean, vertical bar = mean ± one standard deviation).

3. Asymptotic mechanical behaviour of SWNTs with increasing tube length

3.1. Increasing length and its effect on strength

The asymptotic behaviour of the ultimate strength of SWNT with a constant average density of defects as tube length increases is considered in this section. Recall that a tube may be considered to be composed of n segments of length Δ_i for $i = 1, \ldots, n$. The length of the tube, $l_n = \sum_{i=1}^{n} \Delta_i$, depends on n, as does the strength of the tube, $W_{(n)}$:

$$W_{(n)} = \min\{W_1, W_2, \ldots, W_n\} \tag{9}$$

where W_i is the strength of the ith segment. Owing to the presence of random defects and random velocities of the atoms, each W_i is random in nature; consequently $W_{(n)}$ is random as well. It is reasonable to assume that the strength field is statistically homogeneous, hence, if $\Delta_i = l_0$ for each i, then each W_i has the same marginal cumulative distribution function (CDF), F_W.

It is well known that if the W_i are i.i.d. (independent and identically distributed) and possess some very general properties that are satisfied by all common distribution functions, extreme value theory [35] shows that the probability distribution of the minimum, $W_{(n,\mathrm{iid})}$, under appropriate normalization, $v_n(z) = c_n + d_n z$, converges as $n \to \infty$ to

$$P[W_{(n,\mathrm{iid})} \leq v_n] = L_{(n)}(v_n) \to L_c(z) = 1 - \exp[-(1 - cz)^{-1/c}], \qquad 1 - cz > 0 \tag{10}$$

where L_c is one of the three classical asymptotic extreme value distributions and depends on the parameter c. With $c = 0$, L_c is interpreted in the limit as the Gumbel distribution for minima; with $c < 0$, L_c is the Weibull distribution for minima; and with $c > 0$, L_c is the Frechet distribution for minima.

The i.i.d. assumption on strength of the tube segments appears unrealistic, since there is likely to be dependence among strengths of neighbouring segments due to the non-local nature of atomic interactions. Fortunately, the above classical results can be extended to the dependent stationary case as well, as long as the dependence reduces with increasing

J. Stat. Mech. (2006) P06021

separation, i.e. there is no long-range memory effect and there is no clustering of very low values.

This decaying dependence can be formalized by a strong mixing condition applied to minima of stationary sequences. The strong mixing condition on a strictly stationary sequence of random variables $\{W_n\}$ ensures that the sigma-algebras, A and B, generated, respectively, by the sub-sequences $\{W_1, \ldots, W_p\}$ and $\{W_{p+k}, W_{p+k+1}, \ldots\}$, become asymptotically independent as the distance between them (i.e. k) becomes large [36]:

$$|P(\mathsf{A} \cap \mathsf{B}) - P(\mathsf{A})P(\mathsf{B})| < g(k) \to 0, \qquad \text{as } k \to \infty. \tag{11}$$

We now introduce two conditions, $D(u_n)$ and $D'(u_n)$, that help establish limiting distributions of extrema from dependent stationary sequences. The former ensures that there is no long-term memory effect in the sequence, while the latter ensures that there is no clustering of very low values.

Condition $D(u_n)$ is a much weakened version of (and implied by) strong mixing and applies, not to the entire sigma-algebras generated by the subsequences, but only to a certain sequence of events of the type $\{W_i > u_n\}$. The strong mixing requirement above is not essential for the asymptotic distribution of minima to exist—the much weaker condition $D(u_n)$ along with $D'(u_n)$ would suffice, but strong mixing is required for the central limit theorem to hold for partial sums of the sequence and the asymptotic independence between minima and the partial sums of the sequence demonstrated later in the paper.

Define G as the complementary cumulative distribution function (CCDF), $G = 1 - F$, and for brevity denote $G_{i,j,k,\ldots}(u)$ as the joint CCDF of $\{W_i, W_j, W_k, \ldots\}$ at the point $(u, u, u, \ldots)$. After Leadbetter *et al* [36], condition $D(u_n)$ can be stated to hold in the context of asymptotic distribution of minima, if for any integers $1 \leq i_1 < \cdots < i_p < j_1 < \cdots < j_{p'} \leq n$ for which $j_1 - i_p \geq l$ we have

$$|G_{i_1,\ldots,i_p,j_1,\ldots,j_{p'}}(u_n) - G_{i_1,\ldots,i_p}(u_n)G_{j_1,\ldots,j_{p'}}(u_n)| \leq \alpha_{n,l} \to 0, \qquad \text{as } n \to \infty \tag{12}$$

for some sequence $l_n = \mathrm{o}(n)$.

Condition $D'(u_n)$ can be stated to hold for the sequence $\{W_n\}$ if for some given real sequence $\{u_n\}$, we have

$$\limsup_{n \to 0} n \sum_{j=2}^{[n/k]} P\{W_1 < u_n, W_j < u_n\} = 0 \qquad \text{as } k \to \infty \tag{13}$$

where [ ] denotes the integer part.

The importance of conditions $D(u_n)$ and $D'(u_n)$ is that under them the asymptotic distribution of the minima of the dependent sequence is still one of three classical types—Weibull, Gumbel or Frechet (equation (10)), although the convergence is slower than that in the i.i.d. case:

$$P[W_{(n)} \leq v_n] \to \hat{L}_{\mathrm{c}}(z) = 1 - \exp[-\theta(1 - cz)^{-1/c}] \tag{14}$$

where $1 - cz > 0, 0 < \theta \leq 1$. The rate of convergence is governed by the *extremal index*, θ, of the sequence, which is a number between zero and unity. The extremal index is discussed in detail in section 3.2.

J. Stat. Mech. (2006) P06021

Let us now investigate how the distribution of nanotube strength approaches its limiting form as the tube length increases. Of the three limiting distributions, we focus on the Weibull model only since the Weibull model is widely adopted for the 'weakest link' type strength variables for materials and systems across spatial scales and materials. The two parameter Weibull CDF is given by

$$F_X(x) = 1 - \exp\left[-\left(\frac{x}{\omega}\right)^{-k}\right] \tag{15}$$

where x is a realization of random variable X, ω is the scale parameter and k is the shape parameter of the distribution.

We continue with the (6, 6) armchair SWNT configuration and increase its length, l, while keeping the average rate of occurrence of SW defects per unit tube surface area constant ($\lambda = 1.59 \times 10^{-3}$ Å^{-2}, $h = 8$ Å). We start with the smallest length $l_0 = 49.2$ Å, and analyse tubes up to 492 Å long in steps of l_0, $2l_0$, $3l_0$, $4l_0$, $5l_0$, $6l_0$ and $10l_0$. The corresponding loading rates are 2.5, 5.0, 7.5, 10.0, 12.5, 15.0 and 25.0 nm ns^{-1} such that the strain rate is constant. 33 samples are generated for each value of l. Since the tube is prismatic, the cross-sectional area of each segment is equal (denoted by A_0) and all discussion pertaining to tube strength above applies equally well when it is normalized by A_0. We thus adopt the more common stress-based description of mechanical strength here (rather than force based) and present the results in terms of ultimate strength, σ_u, of the nanotubes.

Figure 4 shows the distribution of the 33 samples of the ultimate strength of SWNTs with Stone–Wales defects as the tube length increases from l_0 to $10l_0$ plotted on Weibull probability paper. Probability paper represents a linearized relation between a (typically two parameter) CDF and the random deviate after suitable transformations: it is constructed such that the relative cumulative frequencies (i.e. the observed CDF) from a random sample would plot linearly with the observed data if the sample truly followed the underlying distribution. The quality of Weibull fit clearly appears to improve with increasing tube length in figure 4.

Table 2 shows the quantitative analysis of the same data set as in figure 4. It is clear that the distribution shifts to the left (i.e. the mean decreases) and becomes narrower (i.e. the c.o.v. decreases) with increasing l: this is consistent with the behaviour of extremes from a stationary population. Using the first two moments calculated from the 33 data points, a chi-squared goodness of fit is performed in each case with six equi-probable intervals, i.e. three degrees of freedom. The quality of Weibull fit (judged from the level of significance of the chi-squared test) among this set of data is found to generally improve with increasing l, and is best when $l = 6l_0$.

3.2. The extremal index of the strength field

We now investigate the degree of dependence in the strength field in terms of the extremal index mentioned above. The extremal index, θ, is a positive fraction between zero and one, $0 < \theta \leq 1$. The case of $\theta = 1$ corresponds to the i.i.d. case while the case of $\theta = 0$ is degenerate and implies long range dependence. In the context of characterizing the minima of a stationary sequence, the extremal index may be interpreted as the reciprocal of the

J. Stat. Mech. (2006) P06021

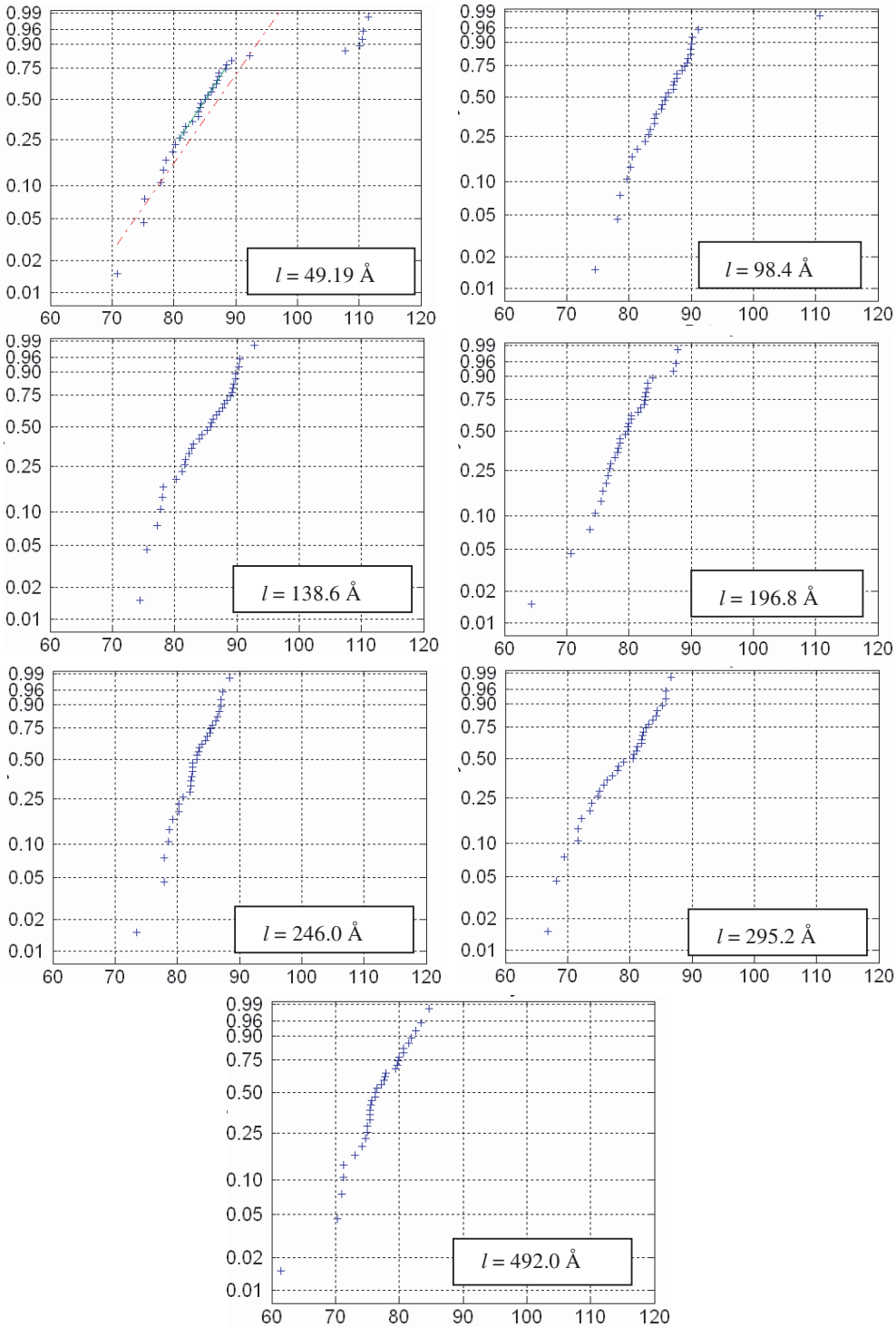

Figure 4. Weibull probability plot for SWNT ultimate strength with increasing tube length (33 samples each; horizontal axis, observed strength in GPa; vertical axis, observed cumulative relative frequency).

J. Stat. Mech. (2006) P06021

Table 2. Statistics of SWNT ultimate strength as a function of tube length. (Based on 33 samples for each l, μ = mean, V = coefficient of variation (s.d./mean).)

n	Tube length, l (Å)	μ (GPa)	V (%)	Weibull parameters		Weibull goodness of fit	
				ω	k	χ^2 statistic	Level of significance
1	49.19	87.30	12.35	91.88	9.73	20.27	1.49×10^{-4}
2	98.38	86.04	6.98	88.66	17.70	11.34	0.2004
3	147.57	84.68	5.74	86.81	21.66	3.18	0.3644
4	196.76	82.89	4.03	84.37	31.09	6.82	0.0779
5	246.0	79.38	5.97	81.46	20.78	3.91	0.2714
6	295.2	78.64	6.95	81.03	17.76	1.73	0.6309
10	492.0	76.63	5.96	78.64	20.81	3.55	0.3149

limiting mean cluster size below a low threshold. This interpretation will be formalized later in obtaining numerical estimates of the extremal index for the carbon nanotubes.

The stationary dependent sequence $\{W_i\}$ with marginal CDF F_W has extremal index θ if for each $\tau > 0$, as $n \to \infty$,

(i) there exists a sequence $v_n(\tau)$ such that $nF_W(v_n(\tau)) \to \tau$, and
(ii) $P[W_{(n)} \geq v_n(\tau)] \to \exp(-\theta\tau)$ where $W_{(n)}$ is given by equation (9).

The extremal index also helps underline the degree of conservatism in making the i.i.d. hypothesis when predicting the distribution of the minima from a random sequence. Equations (10) and (14) clearly show that L_c (obtained from the i.i.d. assumption) and $\hat{L}_c$ (the actual CDF) are not only of the same type for any given value of c, but also for any value of z we always get $L_c > \hat{L}_c$. In other words, the distribution with the i.i.d. assumption is always to the left of the actual (that considers dependence) and thus underpredicts the strength.

From a practical point of view, the utility of the extremal index is that the distribution of the minimum $W_{(n)}$ of a stationary dependent sequence, provided it converges (which can be guaranteed by conditions $D(u_n)$ and $D'(u_n)$), may be estimated, at least in the left tail, simply with the help of the marginal distribution F_W (or, equivalently, its complement, G_W) and the extremal index θ of the underlying process, as

$$P[W_{(n)} \geq u_n] \approx G_W^{n\theta}(u_n) \tag{16}$$

for sufficiently high u_n and large n.

We can then estimate the extremal index if we have the statistics of nanotube strength for known values of n:

$$\hat{\theta} \approx \frac{1}{n} \frac{\ln G_{W(n)}(x)}{\ln G_{W(1)}(x)} \tag{17}$$

where $G_{W(n)}$ is the complementary distribution function of a nanotube of length nl_0. It is apparent from equation (17) that the *estimated* extremal index depends on the threshold x, although what we are ultimately interested in is its limiting value as $x \to 0$. Based on

results from maxima of a stationary dependent sequence [37], we propose the following threshold dependent form for the extremal index:

$$P[M_{2,r} > x | W_1 \leq x] = \theta + R(F_W(x)) \tag{18}$$

where r is an integer denoting 'run length'. This form is regardless of the type of limiting distribution for the sequence (equation (14)). The quantity $M_{p,q} = \min\{W_p, \ldots, W_q\}$ and the residual $R(F_W(x)) \to 0$ as $x \to x_0 = \inf(x : F_W(x) > 0)$. From this representation, the limiting value $\hat{\theta}_0$, at $x = 0$, may be estimated as follows. The error between the estimate $\hat{\theta}(x)$ at some arbitrary threshold $x > 0$ and the limiting estimate $\hat{\theta}_0$ has commonly a log-linear relation with $F_W(x)$:

$$\hat{\theta}(x) = \hat{\theta}_0 + \beta_1 F_W(x)^{\beta_2}, \qquad \beta_1 \neq 0, \qquad \beta_2 > 0, \qquad \text{as } F_W(x) \to 0. \tag{19}$$

For any given n (or equivalently l), the three parameters $\hat{\theta}_0$, β_1 and β_2 can be estimated from the data.

Figure 5 shows the estimated extremal index $\hat{\theta}$ as a function of CDF F_W for tubes of different lengths. The circles show the observed data (as obtained from equation (17)) while the solid line shows the non-linear least-square fit according to equation (19). For any given l, the limiting value of the estimate, $\hat{\theta}_0$, is simply the intercept of the solid line at $F_W = 0$. It is clear that there is a substantial amount of dependence in the strength field, and strengths of the individual segments are clearly not i.i.d.

Figure 6 plots the limiting value $\hat{\theta}_0$ as a function of tube length. A strong dependence in the strength field is suggested in figure 6; the extremal index is seen to approach the numerical value of around 0.16. Costly atomistic simulations will no longer be required for predicting the strength distribution of longer tubes; the extremal index can be used in conjunction with equation (17) to estimate at least the left tail for any value of n. The estimate of θ can also be instrumental in deciphering the underlying correlation structure in the random strength field, although it is outside the scope of this work.

3.3. Compliance statistics and its asymptotic independence from strength

In studying SWNT compliance properties, we continue with the above formulation of a nanotube being composed of n segments of equal length ($\Delta_i = l_0$ for each $i = 1, \ldots, n$), cross-sectional area A_0 and random strength W_i with marginal distribution F (independent of i). The length of the tube, $l_n = \sum_{i=1}^{n} \Delta_i = nl_0$, depends on n as before. The compliance of the entire tube, $C_{(n)}$, as a function of n, can be given as the sum of the individual segment compliances, C_i:

$$C_{(n)} = C_0 + \sum_{i=1}^{n} C_i \tag{20}$$

where C_0 is the contribution from inertial effects. We now make use of the fundamental description of mechanical failure that we have used in atomistic simulation for solids above, namely, fracture of solids is displacement based. An atomic bond is regarded as broken if the inter-atomic separation exceeds the critical value r_f. If the tube segments are small

J. Stat. Mech. (2006) P06021

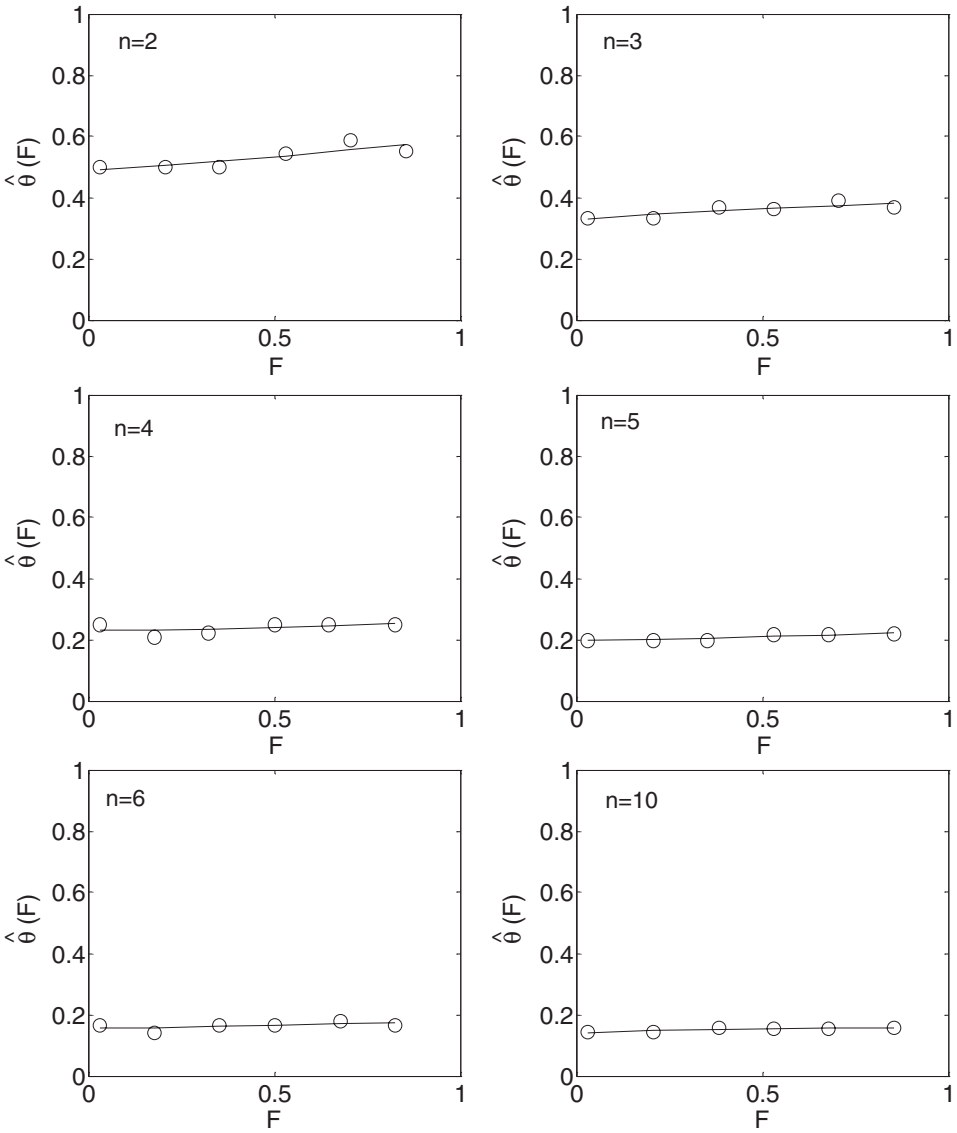

Figure 5. Estimated extremal index as a function of non-exceedance probability, F, for various tube lengths, $l = nl_0$ (circle = observed value equation (17), solid line = fit of equation (19)).

enough, and the static force–displacement behaviour of each segment can be assumed to be linear up to failure, then compliance of each segment may be approximated as

$$C_i = \frac{A_0}{l_0}\frac{\alpha r_f}{W_i} \tag{21}$$

where α is constant for given tube chirality and l_0. The compliance of the entire tube can then be given by

$$C_{(n)} = C_0 + \frac{A_0}{l_0}\alpha r_f \sum_{i=1}^{n} \frac{1}{W_i}. \tag{22}$$

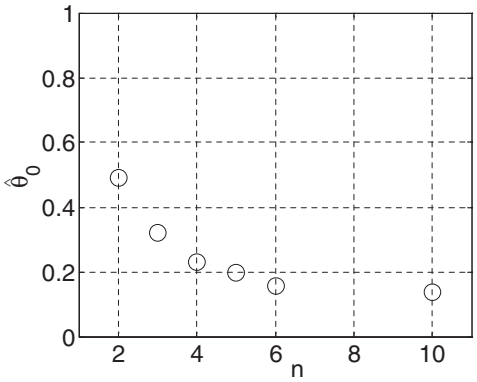

Figure 6. Limiting extremal index as a function of tube length.

Let us now investigate the statistical properties of $C_{(n)}$ as n grows large. If the stationary sequence $\{W_n\}$ is strongly mixing, so is $\{1/W_n\}$. It is known that (i) sums of stationary and strong mixing sequences are asymptotically normal; further, (ii) these sums are asymptotically independent of the extrema of the sequences [38, 39]. It will be instructive to determine how well our results support these two important properties of strong mixing sequences.

Table 3 shows the statistics of the compliance of SWNTs with Stone–Wales defects as a function of tube length, l. The distribution shifts slowly to the right and narrows slightly with increasing l: this is consistent with the behaviour of partial sums from a stationary sequence (equation (22)). We also investigate the goodness of normal fit on the SWNT compliance data as the tube length increases from l_0 to $10l_0$. Using the first two moments calculated from the 33 data points, a chi-squared goodness of fit is performed in each case with six equi-probable intervals, i.e. three degrees of freedom. The goodness of the normal fit is also verified graphically in figure 7. Similar to the Weibull probability paper discussed above, the normal probability paper plots the following linear relation:

$$\Phi^{-1}(\hat{F}_X(x)) = \frac{1}{\hat{\sigma}}x - \frac{\hat{\mu}}{\hat{\sigma}} \tag{23}$$

where $\hat{F}_X(x)$ is the observed CDF of the random variable X, Φ^{-1} is the inverse standard normal distribution function, and $\hat{\mu}$ and $\hat{\sigma}$ are estimates of the first two moments of the distribution. It is clear from table 3 and figure 7 that the accuracy of the normal hypothesis improves as l increases.

Finally, figure 8 shows the correlation coefficient between the compliance and the ultimate strength of the tube as the tube length increases. Consistent with the asymptotic independence of sums and extrema from strong mixing sequences as described above, these quantities are clearly found to become uncorrelated as the tube length becomes large.

4. Summary and conclusions

Defects are commonly present in materials and occur/evolve randomly in space and time, and these defects may have significant effects on the mechanical and other properties. Material properties governed by sums (or averages) of some underlying

J. Stat. Mech. (2006) P06021

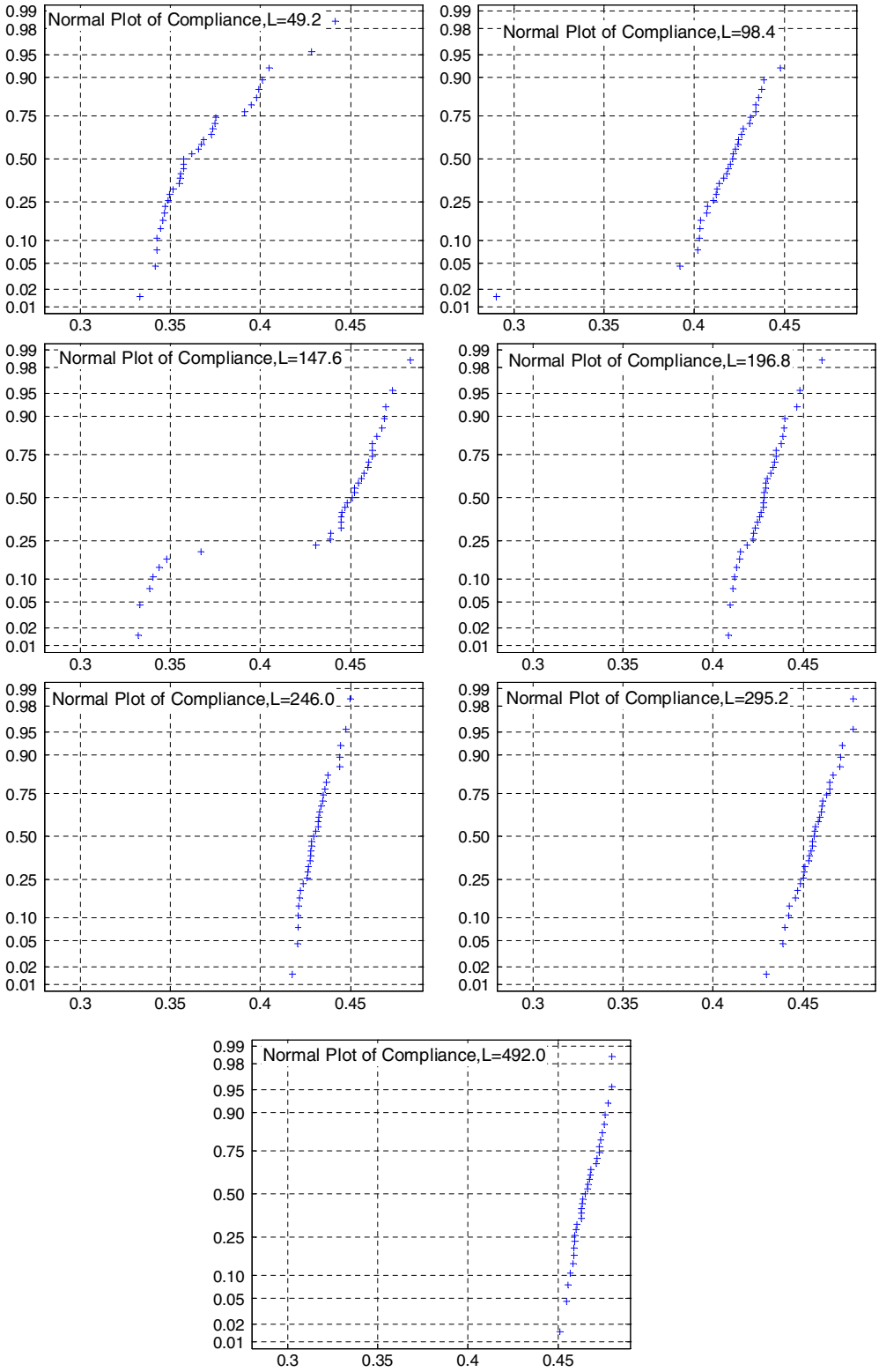

Figure 7. Normal probability plot for SWNT compliance with increasing tube length (33 samples each. Horizontal axis, observed compliance in 1/TPa, vertical axis, observed cumulative relative frequency).

J. Stat. Mech. (2006) P06021

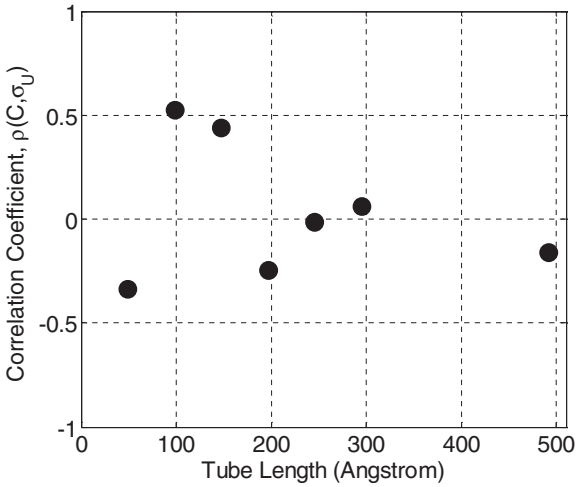

Figure 8. Asymptotic independence of tube strength and compliance.

Table 3. Statistics of SWNT compliance as a function of tube length. (Based on 33 samples for each n, μ = mean, V = coefficient of variation (s.d./mean).)

				Normal goodness of fit	
n	Tube length, l (Å)	μ (1/TPa)	V (%)	χ^2 statistic	Level of significance
1	49.2	0.3682	2.61	8.2727	0.0407
2	98.4	0.4267	5.20	33.7273	2.2620e−007
3	147.6	0.4316	4.81	30.0909	1.3206e−006
4	196.8	0.4281	1.19	2.4545	0.4836
5	246.0	0.4309	0.83	1.7273	0.6309
6	295.2	0.4561	1.12	1	0.8013
10	492.0	0.4660	0.78	1	0.8013

stochastic phenomena can be shown to diverge from and become independent of properties governed by extremes arising of the same phenomena. In this paper we considered the random nature of Stone–Wales (SW) defects in carbon nanotubes (CNTs) and, through the technique of atomistic simulation, quantified the effect of such randomness on the asymptotic behaviour of ultimate strength and compliance as the tube length increases.

The existence of dependence in the ultimate strength random field of the nanotube (that should ideally decrease with increasing separation), consistent with the non-local nature of atomic interactions, was considered; a strong mixing condition was assumed for the field to formalize the dependence structure. Limiting expressions for the distribution of strength as tube length became large was developed. The extremal index, which can be used to characterize the strength of the said dependence, was estimated. The conservatism introduced by the commonly made i.i.d. (independent and identically distributed) assumption was also discussed.

The distribution of ultimate strength, σ_u, and compliance, C, with increasing tube length, l, of (6, 6) armchair SWNTs was investigated. The average rate of occurrence

J. Stat. Mech. (2006) P06021

of SW defects per unit tube surface area was kept constant. Seven values of l spanning an order of magnitude were considered (from 49 to 490 Å) and the loading was adjusted such that the strain rate was the same for each tube length. The strength distribution was found to shift to the left and become narrower with increasing l, and also appeared to fit the Weibull distribution rather well. The distribution of C as the scaled sum of the reciprocal of the strong mixing strength sequence was studied with increasing tube length as well. The compliance of the tube increased with increasing length and became asymptotically normal. Finally, the compliance and strength of the tube were found to be asymptotically uncorrelated. These results appeared to validate the strong mixing property of the strength field. These findings can be used in future studies to better model the random mechanical behaviour of nanotubes and nanotube based devices.

Acknowledgment

A small set of preliminary results from this work was presented at the Ninth International Conference on Structural Safety and Reliability held in Rome, Italy, in June 2005.

References

[1] Kingman J F C, 1993 *Poisson Processes* (New York: Oxford University Press)
[2] der Kiureghian A and Zhang Y, *Space-variant finite element reliability analysis*, 1999 *Comput. Methods Appl. Mech. Eng.* **168** 173
[3] Iijima S, *Helical microtubules of graphitic carbon*, 1991 *Nature* **354** 56
[4] Iijima S *et al*, *Pentagons, heptagons and negative curvature in graphite microtubule growth*, 1992 *Nature* **356** 776
[5] Terrones M, *Science and technology of the twenty-first century: synthesis, properties, and applications of carbon nantoubes*, 2003 *Ann. Rev. Mater. Res.* **33** 419
[6] Dresselhaus M S and Dai H, *Carbon nanotubes: Continued innovations and challenges*, 2004 *MRS Bull.* **29** 237
[7] Salvetat J P *et al*, *Mechanical properties of carbon nanotubes*, 1999 *Appl. Phys.* A **69** 255
[8] Yakobson B I and Avouris P, *Mechanical properties of carbon nanotubes*, 2001 *Top. Appl. Phys.* **80** 287
[9] Bernholc J *et al*, *Mechanical and electrical properties of nanotubes*, 2002 *Ann. Rev. Mater. Res.* **32** 347
[10] Lu Q and Bhattacharya B, *Effect of randomly occurring Stone–Wales defects on mechanical properties of carbon nanotubes using atomistic simulation*, 2005 *Nanotechnology* **16** 555
[11] Chandra N *et al*, *Local elastic properties of carbon nanotubes in the presence of Stone–Wales defects*, 2004 *Phys. Rev.* B **69** 094101
[12] Sears A and Batra R C, *Macroscopic properties of carbon nanotubes from molecular-mechanics simulations*, 2004 *Phys. Rev.* B **69** 235406
[13] Zhou O *et al*, *Defects in carbon nanostructures*, 1994 *Science* **263** 1744
[14] Charlier J C, *Defects in carbon nanotube*, 2002 *Acc. Chem. Res.* **35** 1063
[15] Ouyang M *et al*, *Atomically resolved single-walled carbon nanotube intramolecular junctions*, 2001 *Science* **291** 97
[16] Lu Q and Bhattacharya B, *The role of atomistic simulations in probing the small-scale aspects of fracture—a case study on a single-walled carbon nanotube*, 2005 *Eng. Fract. Mech.* **72** 2037
[17] Mielke S L *et al*, *The role of vacancy defects and holes in the fracture of carbon nanotubes*, 2004 *Chem. Phys. Lett.* **390** 413
[18] Nardelli M B *et al*, *Mechanism of strain release in carbon nanotube*, 1998 *Phys. Rev.* B **57** R4277
[19] Yakobson B I, *Mechanical relaxation and intramolecular plasticity in carbon nanotubes*, 1998 *Appl. Phys. Lett.* **72** 918
[20] Liew K M *et al*, *On the study of elastic and plastic properties of multi-walled carbon nanotubes under axial tension using molecular dynamics simulation*, 2004 *Acta Mater.* **52** 2521
[21] Jiang H *et al*, *Defect nucleation in carbon nanotubes under tension and torsion: Stone–Wales transformation*, 2004 *Comput. Methods Appl. Mech. Eng.* **193** 3419
[22] Samsonidze G G *et al*, *Kinetic theory of symmetry-dependent strength in carbon nanotubes*, 2002 *Phys. Rev. Lett.* **88** 065501

J. Stat. Mech. (2006) P06021

[23] Zhao Q *et al*, *Ultimate strength of carbon nanotubes: a theoretical study*, 2002 *Phys. Rev.* B **65** 144105
[24] Zhou L G and Shi S Q, *Formation energy of Stone–Wales defects in carbon nanotubes*, 2003 *Appl. Phys. Lett.* **83** 1222
[25] Saether E, *Transverse mechanical properties of carbon nanotube crystals. Part II: sensitivity to lattice distortions*, 2003 *Compos. Sci. Technol.* **63** 1551
[26] Belavin V V *et al*, *Modifications to the electronic structure of carbon nanotubes with symmetric and random vacancies*, 2004 *Int. J. Quant. Chem.* **96** 239
[27] Matern B, 1986 *Spatial Variation* (*Lecture Notes in Statistics* vol 36) (Berlin: Springer)
[28] Lu Q, *Influence of random defects on the mechanical behaviour of carbon nanotubes through atomistic simulation*, 2005 *PhD Thesis* Civil and Environmental Engineering Department. Newark, DE, University of Delaware
[29] Belytschko T *et al*, *Atomistic simulations of nanotube fracture*, 2002 *Phys. Rev.* B **65** 235430
[30] Dumitrica T *et al*, *Bond-breaking bifurcation states in carbon nanotube fracture*, 2003 *J. Chem. Phys.* **118** 9485
[31] Troya D *et al*, *Carbon nanotube fracture—differences between quantum mechanical mechanisms and those of empirical potentials*, 2003 *Chem. Phys. Lett.* **382** 133
[32] Brenner D W, *Empirical potential for hydrocarbons for use in simulating the chemical vapor deposition of diamond films*, 1990 *Phys. Rev.* B **42** 9458
[33] Lu Q and Bhattacharya B, 2005 *Analysis of Randomness in Mechanical Properties of Carbon Nanotubes through Atomistic Simulation* (*46th AIAA/ASME/ASCE/AHS/ASC Structures, Structural Dynamics & Materials Conf.*) Austin, TX
[34] Lu Q and Bhattacharya B, *Fracture resistance of zigzag single-walled carbon nanotubes*, 2006 *Nanotechnol. Institute of Phys.* **17** 1323
[35] Galambos J, 1987 *The Asymptotic Theory of Extreme Order Statistics* (Malabar, FL: Krieger)
[36] Leadbetter M R *et al*, 1983 *Extremes and Related Properties of Random Sequences and Processes* (New York: Springer)
[37] Hsing T, *Extremal index estimation for a weakly dependent stationary sequence*, 1993 *Ann. Stat.* **21** 2043
[38] Anderson C W and Turkman K F, *The joint limiting distribution of sums and maxima of stationary sequences*, 1991 *J. Appl. Probab.* **28** 33
[39] Hsing T, *On the asymptotic independence of the sum and rare values of weakly dependent stationary random variables*, 1995 *Stoch. Process. Appl.* **60** 49